In situ X-ray diffraction under H2 of the pseudo-AB2 compounds: YNi3.5Al0.5Mg

Cristina Stan, Ecaterina Andronescu, Kohta Asano, Kouji Sakaki, Jean-Louis Bobet

In situ X-ray diffraction under H_2 of the pseudo-AB_2 compounds: $YNi_{3.5}Al_{0.5}Mg$

Cristina Stan , Ecaterina Andronescu , Kohta Asano , Kouji Sakaki , Jean-Louis Bobet

1. Introduction

Magnesium is promising for hydrogen storage applications due to its high hydrogen capacity (i.e. 7.6 wt% of hydrogen), high resources and low cost [1]. The main disadvantages of MgH_2 as a hydrogen storage media are the high temperature of hydrogen discharge, the slow desorption kinetics and the high reactivity towards air and oxygen [2] and [3]. In order to head off the poor reaction kinetics of the Mg, ball milling was used to modify the Mg surface. Metals, alloys and oxides [1] were also added to improve the kinetics (mainly by improving the dissociation of H_2). Nevertheless, if the kinetics can be improved on that way, the thermodynamic remains unchanged [4], [5], [6], [7], [8], [9] and [10].

On the other hand, the Laves phases AB_2 have been extensively studied as it exhibits reversible hydriding properties around room temperature and atmospheric pressure. However, the maximum hydrogen capacity is limited to about 1.5 wt%. Combining the advantages of both Mg and AB_2 compounds has been studied but the results are not as promising as expected [11], [12], [13], [14] and [15]. Therefore, $RE_{1-x}Mg_xNi_2$ has been studied recently [16], [17], [18] and [19].

Typical hydrogen-absorbing alloys used for hydrogen storage show the following phase transition in the hydriding reaction: alloy → solid solution of hydrogen in the alloy (*phase) → solid solution and hydride phases (two phases co-existing) → solution solid of hydrogen in hydride phase (β phase). The dehydriding reaction phase transition follows the reverse process of the hydriding. This is usually represented as a Pressure Composition isotherms (i.e. PCi) curves.

Hydrogen absorbing and desorbing properties of metal hydrides are closely related to the crystal structure. However, the number of reported crystal structures of hydride phases are not so large [20] and [21] because of the difficulty of measurements. Equilibrium pressure and hydrogen capacity are well known as hydrogen absorbing properties, and they can be controlled by the crystal structure or atomic arrangement around the hydrogen site.

For that reason, the in situ XRD measurements is a conventional and suitable method and provide substantial information such as the structure changes in metal lattice, the symmetry, the lattice parameters, the lattice strain and the crystallinity.

In a previous paper [22], a series of intermetallic compounds in the YNi4-xAlxMg systems were prepared and the relationship between the structure and the hydrogen sorption properties was established. Among all the compounds, $YNi_{3.5}Al_{0.5}Mg$ showed the most interesting properties as the equilibrium pressure at room temperature was close to 1 bar.

This paper presents the results of in situ XRD measurements of $YNi_{3.5}Al_{0.5}Mg$ along the P–C isotherm. The evolution of the lattice strain, the crystallite size and lattice parameters in both metal and hydride phases, during the hydriding–dehydriding process are investigated.

2. Experimental details

The $YNi_{3.5}Al_{0.5}Mg$ was prepared by ball milling [22], starting from the pure elemental powders of Y, Ni, Al and Mg (purity$\geqslant$99.5%). After milling process, the powders were thermally treated at 650 °C under argon atmosphere for 1 h to obtain a well-crystallized compound.

The chemical composition and homogeneity of the sample were investigated by electron microprobe analysis with a CAMECA SX-100 instrument. Characterisation of the structure and identification of the phases were done by X-ray powder diffraction using a Philips PW 1050 diffractometer with Cu K_* radiation. Hydrogen sorption properties were investigated with the use of an automatic Sievert-type volumetric apparatus [23].

In situ XRD measurements were performed using a vertical type diffractometer (Rigaku, RINT-2500V) equipped with a rotating Cu anode, a high-pressure chamber and a temperature controller. The powder sample was filled onto a stainless-steel sample holder and covered with a beryllium film. A thermocouple was inserted into the sample holder to monitor the sample temperature [24]. The sample was kept at constant temperature for 1 h and it was measured at room temperature. XRD data were measured along the P–C isotherms of the sample itself: for example, in hydriding, hydrogen gas was introduced to the chamber from a reservoir with a known volume and the XRD profile was measured after the pressure in the chamber reached equilibrium.

3. Results and discussion

Fig. 1 shows absorption and desorption P–C isotherms of $YNi_{3.5}Al_{0.5}Mg$ measured at room temperature. XRD profiles were measured at each of the indicated points on the P–C

isotherms (e.g. seven points on absorption and six points in the desorption process).

As an example, XRD profiles for the $YNi_{3.5}Al_{0.5}Mg$ in the absorption process (A4) and in the desorption process (D1) are shown in Fig. 2. These two points (i.e. A4 and D1) are in the plateau region so that the sample consists of a mixture of both $*$ and β phases. On these XRD patterns it is possible to index the peaks of both phases: the metal ($*$ phase) and the metal hydride (β phase) phases, respectively. Therefore, for the lower 2θ value, the peaks relative to both phases are so close that a mathematical deconvolution of the peak has to be used to identify both peaks. To simplify, a Gaussian profile was used for the deconvolution instead of a pseudo Voigt function. The parameters calculated for the metal ($*$phase) are presented in Table 1 and the results of the hydride phase (β phase) in Table 2, along the PCi. It is therefore worth pointing out that the relative amount of $*$ phase for A6 and D1 experiments as well as the relative amount of the β phase for D2, D3 and D4 is relatively low so that the accuracy of these data is poor (so that the results were not taken into account for discussion).
As shown previously [22], on XRD patterns, some small peaks cannot be indexed on the basis of pseudo-AB2 compound. This result is in good agreement with the EPMA analysis where some YNi_5 type compounds can be detected. However, the sample is homogeneous and the composition of the major phase is close to the nominal composition.

The Williamson and Hall [25] plots for $YNi_{3.5}Al_{0.5}Mg$ deduced from the in situ XRD measured along the P–C isotherms are shown in Fig. 3 and Fig. 4 (point A1 for the initial compound and A4 for β phase in Fig. 3 and point D1, $*$ and β phases, in Fig. 4). Silicon was used prior to the experiment to estimate the peak broadening induced by the apparatus. The Caglioti law calculated for silicon was

$$0.0327\tan^2\theta - 0.0614\tan\theta + 0.0384 = (\mathrm{FWHM})^2.$$

Such relation was used to calculate the apparatus peak broadening at all θ angles. As previously mentioned Gaussian profile was used to fit the XRD patterns and so the integral width of the sample was calculated as follows:

$$\beta_{\mathrm{sample}} = (\beta^2_{\mathrm{exp}} - \beta^2_{\mathrm{Si(ref)}})^{1/2}.$$

In the case of a Gaussian profile, the relation between the integral width (β) and the Full Width at Half Maximum (FWHM) is

FWHM=β×2(ln2/π)1/2.

Lattice strain and crystallite size for each phase in the absorption–desorption process were calculated (Table 1 and Table 2) from these Williamson and Hall plots. As a matter of comparison, the value obtained with the Scherrer formula (i.e. L=0.9λ/βcosθ) for the

(3 1 1) plane are also given in the tables.

As expected (see for example [26]), it can be noticed than the crystallite size determined with the Scherrer formula is generally lower than the one determined from the Williamson and Hall plot.

The sample used for the experiments has been submitted to three hydrogen absorption–desorption cycles prior to the in situ XRD measurements. Therefore, the crystallite size measured at the beginning (i.e. point A1 on the PCi) is only 376 Å which is lower than the one determined for the as-cast material (i.e. $L_{(Scherrer)} \sim 750$ Å). This reveals that the subsequent hydrogen sorption cycles lead to a decrease of the crystallinity.

From Table 1, it is observed that during the absorption, the crystallite size of the $*$ phase decreases (almost by a factor of 2) meanwhile it remains almost constant during the desorption process. Such variation cannot be linked with the variation of the lattice strain which remains almost constant during both absorption and desorption processes (e.g. the values for A6 and D1 are not significant because of the poor accuracy).

The β phase behaves in a different manner. During the absorption process, the crystallite size remains almost constant meanwhile the lattice strain decreases. It is even noticeable that the lattice strain is high at the beginning and decreases very rapidly to tend to zero at the end of the desorption process. The decrease of the lattice strain during the desorption has to be correlated with the decrease of the crystallite size (by a factor of 2 during the desorption process). This can be explained by the release of hydrogen from the materials.

It was already observed in the case of some AB_2 compounds that the hydrogenation can lead to the amorphisation of the compound. Aoki et al. have demonstrated that the atomic size ratio RA/RB is the dominant factor for controlling the occurrence of such hydrogen induced amorphisation (HIA) and also that compounds with the ratio above 1.37 are amorphised upon hydrogenation [27] and [28]. The RA and RB are the Goldschmidt radii of the A and B atoms in AB2 Laves phase structure, respectively.

For $YNi_{3.5}Al_{0.5}Mg$, the metallic radii are 1.801, 1.60, 1.246 and 1.43 for Y, Mg, Ni and Al, respectively. Considering a random mixture of Ni and Al on the 16e site, the B radius can be taken as equal to 1.269 Å (i.e. 1.246×3.5/4+1.43×0.5/4). Then, *RA/RB* is equal to 1.42 with Y (i.e. considering the A atoms as Y) or 1.26 with Mg. A decrease of the crystallinity is noticed here but it cannot be considered as an amorphisation. If the 4a and 4c sites would be occupied randomly by Mg and Y atoms, then the average A radius would be 1.70 Å (i.e. (1.801+1.60)/2). In such a case, *RA/RB* would be equal to 1.34 and the amorphisation should occur according to the Aoki criteria. As no amorphisation is observed, it is demonstrated that the 4a and 4c sites are not randomly occupied by Mg

and Y as reported in [22] and [29]. The criteria defined by Aoki et al. are easily applicable for AB_2 compounds but not for pseudo-AB2 compounds. Finally, it is worth pointing out that Guénée et al. [30] reported a change in the structure from the cubic form to the orthorhombic one after hydrogenation. Recently, Prigent and Gupta [31] also demonstrated by ab initio calculation that the structure of the $YMgNi_4$ hydride should become orthorhombic. The enthalpy of formation calculated in this case is in good agreement with the experimental value of Aono et al. [16]. Nevertheless, the experiments reported in this paper clearly show that the structure of the hydride can be perfectly indexed with a cubic (F-43m) structure type. The structure of the hydrogenated YNi_4Mg obtained by Aono et al. [16] is different from the hydride synthesised here. The partial substitution of Al to Ni probably helps to retain the cubic structure of the * phase after the hydride formation. The possible decrease of the elastic modulus caused by the Al substitution can be a reason for keeping the cubic structure. As the difference of calculated enthalpy of formation [31] of both the cubic and the orthorhombic hydrides is very different (i.e. -3.3 and $-37.7\,\mathrm{kJ/mol\,H_2}$), it should be assumed that the site occupancy (i.e. $[YNi_2Mg]$) taken into account for the calculation for hydrogen may be incorrect. Some in situ neutrons diffraction will be done in the near future to clarify this point. Another difference can come from the synthesis method and then the defects induced by ball milling can have an effect on the structure of the hydride.

Fig. 5 highlights the plot of cell parameter versus hydrogen pressure along the absorption–desorption process. Lattice parameter of the solid solution phase (i.e. * phase) increases in the single-phase region and it is constant in the two-phase region. Almost the same behaviour is noticed for the β phase. The single * and β phase region corresponds to a solid solution of hydrogen in metal and metal hydride and so the lattice parameter vary almost linearly in the solid solution range and remain constant in the two-phase region (presence of two angular points in the Vegard diagram).

This result is as expected and is in relative good agreement with the previous work of Nakamura et al. [32]. In the * and β regions, the lattice parameter of * and β phases increases to about 5% (from 7.02 to 7.06 and from 7.21 to 7.25 Å for * and β phases, respectively). As the solubility of H in both * and β phases is relatively limited (according to the PCi curves), such huge increase is somewhere unexpected.

Finally, the anisotropic behaviour revealed in the case of AB_5 compounds is not observed here which has to be correlated with the cubic (isotropic) structure.

4. Conclusion

Crystallite size and lattice strain of $YNi_{3.5}Al_{0.5}MgH_x$ during the sorption process were investigated by in situ X-ray powder diffraction. The effectiveness of in situ measurement has been clearly shown because the contact between the hydride and alloy phases at the two-phase region was observed, which ex situ measurements could not follow.

Concerning the variation of crystallinity and micro deformation in the $YNi_{3.5}Al_{0.5}Mg$ compound, it can be concluded that the crystallite size decreases during the absorption for the $*$ phase as the lattice strain remains constant (e.g. during both absorption and desorption). For the β phase, the crystallite size remains almost constant during the absorption and decreases during the desorption. The internal strain are relaxed during the desorption. Finally, it is observed that the structure of $YNi_{3.5}Al_{0.5}Mg$ remains cubic during the sorption process.

Acknowledgements

The authors acknowledge the financial support from (i) CNRS and AUF (Ph.D. grant to Cristina Stan) and (ii) AIST-NEDO from Japan through a project on hydrogen storage. The authors also address special thanks to Prof. Akiba for allowing to use his in situ XRD equipment in AIST Laboratory in Japan.

References

[1] L. Schlapbach and A. Züttel, Nature 414 (2001), pp. 353–358. Full Text via CrossRef | View Record in Scopus | Cited By in Scopus (839)

[2] A. Zaluska, L. Zaluski and J.O. Ström-Olsen, J Alloys Compd 288 (1999), pp. 217–225.

[3] G. Barkhordarian, T. Klassen and R. Bormann, J Alloys Compd 364 (2004), pp. 242–246.

[4] J.-L. Bobet, S. Desmoulins-Krawiec, E. Grigorova, F. Cansell and B. Chevalier, J Alloys Compd 351 (2003), pp. 217–221.

[5] D.S. Lee, I.H. Kwon, J.-L. Bobet and M.Y. Song, J Alloys Compd 366 (1–2) (2004), pp. 279–288.

[6] J. Huot, J.-F. Pelletier, L.B. Lurio, M. Sutton and R. Schultz, J Alloys Compd 348 (1–2) (2003), pp. 319–324.

[7] I.G. Konstanchuk, E.Y. Ivanov, M. Pezat, B. Darriet, V.V. Boldyrev and P. Hagenmuller, J Less-Common Met 131 (1987), p. 181.

[8] G. Alefed and J. Volkl, Hydrogen in metals, Springer, Berlin (1978) p. 1.

[9] J.-L. Bobet, B. Chevalier, M.Y. Song, B. Darriet and J. Etourneau, J Alloys Compd 336 (2002), p. 292.

[10] W. Oelerich, T. Klassen and R. Bormann, J Alloys Compd 322 (2001), pp. L5–L9.

[11] B. Darriet, M. Pezat, A. Hbika and P. Hagenmueller, J Hydrogen Energy 5 (1980), p. 178.

[12] M. Khrussanova, M. Terzieva and P. Peshev, J Less-Common Met 125 (1986), p. 117.

[13] Bobet J-L, Huot J, Roquefere J-G, Baduel S. J Alloys Compd 2008, doi:10.1016/j.jalcom.2008.01.136.

[14] H. Oesterreicher and H. Bitter, J Less-Common Met 73 (1980), pp. 339–344.

[15] K. Kadir, D. Noreus and I. Yamashita, J Alloys Compd 345 (2002), pp. 140–143.

[16] K. Aono, S. Orimo and H. Fujii, J Alloys Compd 309 (2000), pp. L1–L4.

[17] Z.M. Wang, H.Y. Zhou, G. Cheng, Z.F. Gu and A.B. Yu, J Alloys Compd 377 (2004), pp. L7–L9.

[18] Z.M. Wang, H.Y. Zhou, Z.F. Gu, G. Cheng and A.B. Yu, J Alloys Compd 381 (2004), pp. 234–239.

[19] Z.M. Wang, H.Y. Zhou, Z.F. Gu, G. Cheng and A.B. Yu, J Alloys Compd 384 (2004), pp. 279–282.

[20] F. Gingl, L. Gelato and K. Yvon, J Alloys Compd 253–254 (1997), p. 286.

[21] E. Akiba, H. Enoki and Y. Nakamura, Mater Sci Eng A329–331 (2002), pp. 321–324.

[22] Stan C, Andronescu E, Predoi D, Bobet J-L. J Alloys Compd 2007, doi:10.1016/j.jalcom.2007.07.064.

[23] Schultz R, Boily S, Huot J. Canadian Patent, 1999. Ser.-Nr. 2207149.

[24] Y. Nakamura and E. Akiba, J Alloys Compd 345 (2002), pp. 175–182.

[25] H.P. Klug and L.E. Alexander, X-ray diffraction procedures for polycrystalline and amorphous materials (2nd ed.), Wiley, New York, NY (1974) p. 618–87.

[26] S. Vives, E. Gaffet and C. Meunier, Mater Tech 10–12 (2004), pp. 9–13.

[27] K. Aoki, X.-G. Li and T. Masumoto, Acta Metall Mater 40 (7) (1992), p. 1717.

[28] K. Aoki and T. Masumoto, J Alloys Compd 194 (1993), p. 251.

[29] J.-L. Bobet, P. Lesportes, J.-G. Roquefere, B. Chevalier, K. Asano and K. Sakaki et al.,

Int J Hydrogen Energy 32 (2007), pp. 2422–2428.

[30] L. Guénée, V. Favre-Nicolin and K. Yvon, J Alloys Compd 348 (2003), p. 129.

[31] J. Prigent and M. Gupta, J Alloys Compd 446–447 (2007), pp. 90–95.

[32] Y. Nakamura, T. Nomiyama and E. Akiba, J Alloys Compd 413 (2006), pp. 54–62.

Figures

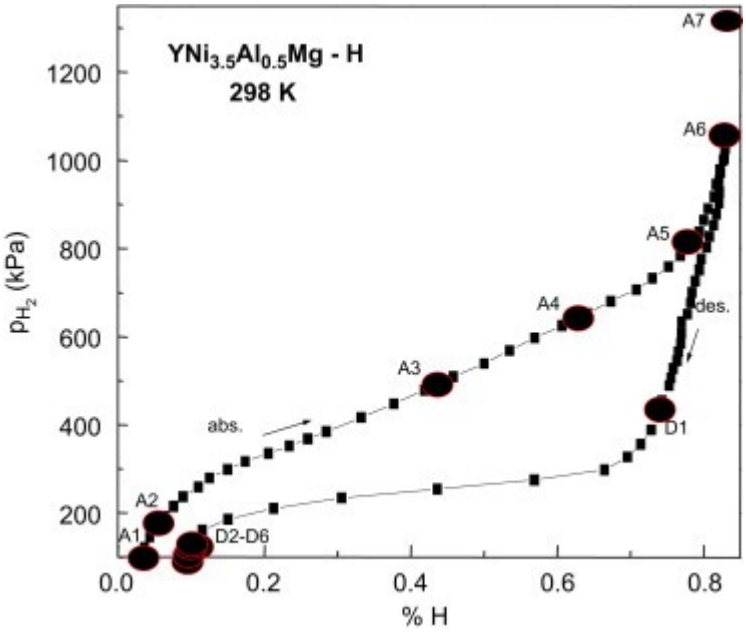

Fig. 1. *P–C* isotherms measured for $YNi_{3.5}Al_{0.5}Mg$ compound and relative point of the in situ XRD analysis.

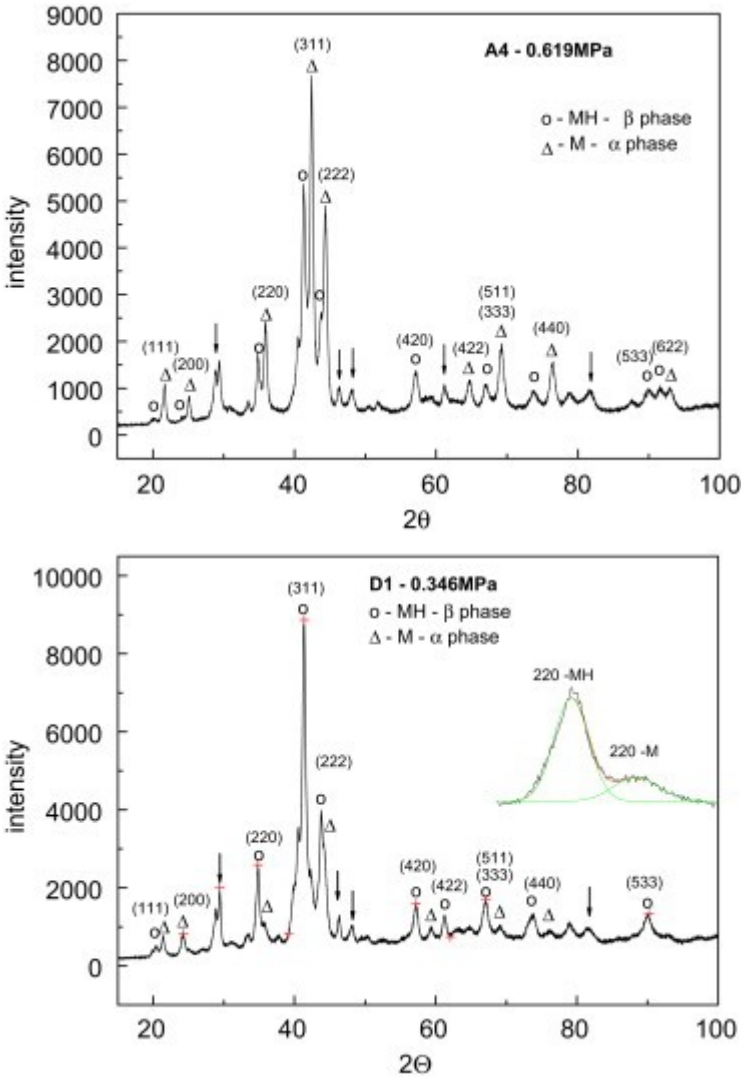

Fig. 2. In situ XRD profiles for $YNi_{3.5}Al_{0.5}Mg$ in absorption process (A4, on the top) and desorption process, respectively (D1, on the bottom). Arrows indicate the presence of YNi_5 impurities.

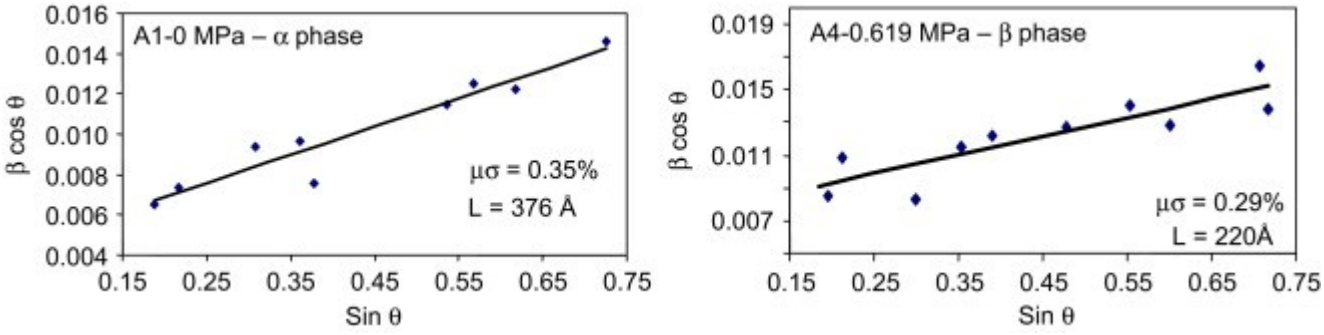

Fig. 3. Williamson and Hall plot during the absorption process for $*$ phase at $P_{H_2} = 0\,\mathrm{MPa}$ on the left (i.e. A1 point on the PCi) and for the β phase at $P_{H_2} = 0.619\,\mathrm{MPa}$ (i.e. point A4 on the PCi) on the right.

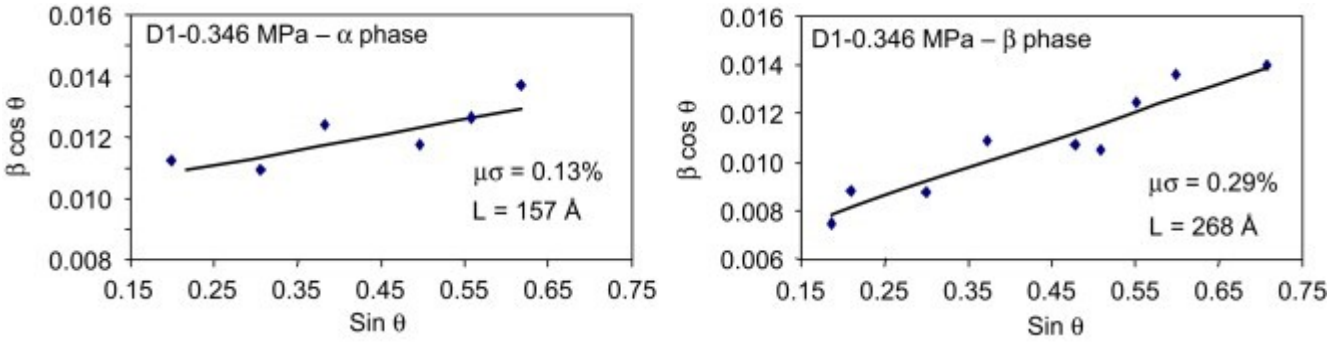

Fig. 4. Williamson and Hall plot for $YNi_{3.5}Al_{0.5}Mg$ during the desorption for * phase on the left and for the *β* phase on the right (i.e. $P_{H_2} = 0.346\,MPa$, point D4 on the PCi).

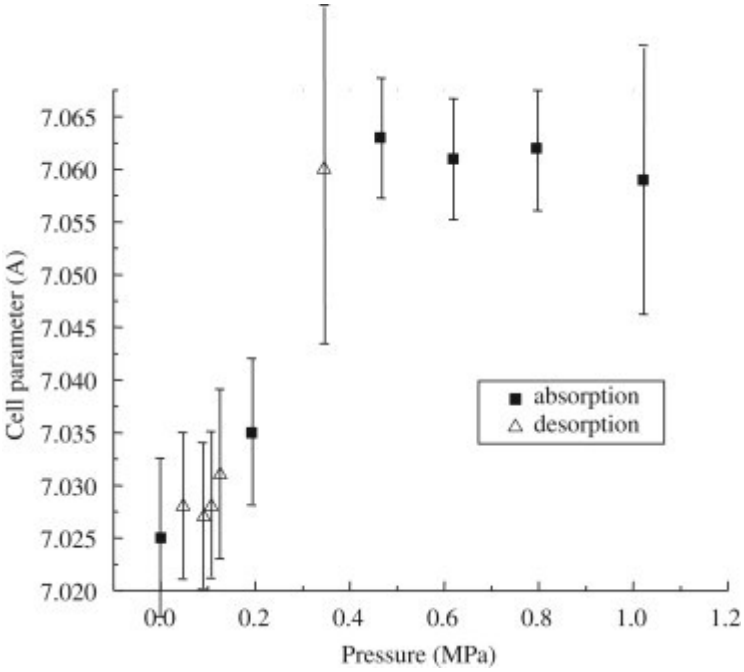

Fig. 5. Cell parameters of $YNi_{3.5}Al_{0.5}Mg$ solid solution phase during the absorption–desorption plotted versus hydrogen pressure.

Tables

Table 1.

Lattice parameter, lattice strain and crystallite size of $YNi_{3.5}Al_{0.5}Mg$ metal (i.e. $*$) phase

Sample	P (MPa)	a (Å)	L (Å)	$\mu\sigma$ (%)	$L_{Scherrer}$
A1	0	7.025±0.008	376 (26)	0.35 (3)	464
A2	0.192	7.035±0.007	336 (31)	0.32 (3)	297
A3	0.464	7.063±0.006	282 (22)	0.34 (2)	261
A4	0.619	7.061±0.006	251 (43)	0.37 (2)	201
A5	0.795	7.062±0.006	178 (18)	0.40 (5)	141
A6[a]	1.021	7.059±0.019	168 (32)	0.46 (9)	131
D1[a]	0.346	7.060±0.021	157 (34)[b]	0.13 (9)[b]	142
D2	0.126	7.031±0.009	182 (22)	0.39 (4)	137
D3	0.107	7.028±0.007	183 (17)	0.37 (3)	131
D4	0.091	7.027±0.007	175 (14)	0.39 (4)	136
D5	0.047	7.028±0.007	175 (17)	0.36 (3)	122

[a] The relative amount of $*$ phase is very low.

[b] Poor accuracy, data not taken into account in the discussion.

Table 2.

Lattice parameter, lattice strain and crystallite size of $YNi_{3.5}Al_{0.5}Mg$ hydride (i.e. β) phase

Sample	P (MPa)	a (Å)	L (Å)	$\mu\sigma$ (%)	$L_{Scherrer}$
A3	0.464	7.202±0.012	230 (14)	0.69 (8)	112
A4	0.619	7.208±0.014	220 (10)	0.29 (3)	121
A5	0.795	7.239±0.014	223 (17)	0.28 (5)	133
A6	1.021	7.218±0.017	219 (18)	0.27 (3)	141
A7	1.333	7.239±0.017	227 (21)	0.31 (4)	139
D1	0.346	7.248±0.018	268 (32)	0.29 (3)	136
D2[a]	0.126	7.205±0.019	151 (19)	0.12 (5)	109
D3[a]	0.107	7.211±0.027	112 (21)	−0.08 (7)	79
D4[a]	0.091	7.208±0.029	102 (22)	0.04 (6)	67

[a] The relative amount of the β phase is very low.